Radiation-induced attenuation self-compensating effect in super-fluorescent fiber source*

Yang Yuan-Hong(杨远洪)[a)b)†], Suo Xin-Xin(索鑫鑫)[a)], and Yang Wei(杨 巍)[b)]

[a)] *Key Laboratory on Precision Opto-mechatronics Technology of Ministry of Education, Beihang University, Beijing* 100191, *China*
[b)] *National Key Laboratory on Inertial Technology, Beihang University, Beijing* 100191, *China*

(Received 13 March 2014; revised manuscript received 16 June 2014; published online 23 July 2014)

The compact super-fluorescent fiber source (SFS) output spectra variations at different pump currents and under different dose of gamma-ray radiation were measured and compared respectively. The radiation-induced attenuation (RIA) self-compensating effect in SFS based on photo-bleaching was found and the general mathematic model of SFS output spectra variations was made. The radiation-induced background attenuation (RIBA) at the pump wavelength was identified to be the main cause of the total output power and spectra variations and the variations can then be compensated by active control of the pump power to enhance the self-compensating effect. With closed-loop feedback control of pump current, double-pass backward (DPB) configuration and spectrum re-shaping technology, an SFS prototype was made and tested. The mean-wavelength stability of about 87.4 ppm and output power instability of less than 5% were achieved under up to 200 krad (Si) gamma-ray irradiation.

Keywords: super-fluorescent fiber source, Er-doped fiber, radiation-induced attenuation, mean wavelength stability

PACS: 42.88.+h, 42.81.wg, 42.81.pa **DOI:** 10.1088/1674-1056/23/9/094213

1. Introduction

Erbium-doped fibers (EDFs) are promising technologies for a number of photonic devices such as super-fluorescent fiber sources (SFSs), fiber lasers and erbium-doped fiber amplifiers. Compared with their semiconductor counterparts, these fiber-optic devices have advantages of higher reliability and lower thermal sensitivity, and have been widely used in optical fiber communication and sensor systems. Recently, there is a growing interest in applying EDF-based devices to space systems, including amplifiers for optical inter-satellite links, SFSs for interferometer fiber-optic gyroscopes (IFOGs), laser altimetry and light detection and ranging systems.[1–3] For space applications, various space rays and ionization radiations were recognized to affect the optical properties of EDFs as well as other waveguide components significantly, so the development of radiation-resistant fiber optic components and systems becomes an important issue for such applications.[4] Specifically, there are critical requirements on the stabilities of output power and mean-wavelength of the SFSs when they are used in IFOGs in order to achieve lower bias drift and maintain a constant scale factor.[5]

To improve the radiation resistant capability of SFSs, a number of approaches were reported such as shielding the EDF by employing heavy metals[6] and using H_2-loaded EDF[7,8] to reduce the radiation-induced attenuation (RIA), tailoring the spectrum[9] to reduce the output spectrum variation. An increase of light power conducted in irradiated fibers can reduce the RIA of the EDF and speed up the power recovery significantly, which is usually designated as photo-bleaching and widely used to improve the stabilities of output power and mean-wavelength.[10,11] Peng *et al.* proposed a complicated closed-loop reflectivity-tuning method to reduce the mean-wavelength drift.[12,13] Modeling and experimental studies showed that RIA depends not only on the total radiation dose, but also on the dose rate, operating optical wavelength, and so on.[14–17] The RIA spectrum may be regarded as the result from the combined contributions of radiation-induced background attenuation (RIBA) and radiation-induced active band attenuation (RIABA). RIBA is due to the generation of a color center with absorption peak generally lying in the ultraviolet region; it can be described with a Lorentzian tail in which the absorption decreases with wavelength increasing. RIABA may depend mainly on the radiation-induced Er^{3+} fluorescent spectrum (active band of EDF) changes.

In this paper, we experimentally studied the SFS output spectra variations at different pump currents and under different doses of gamma-ray radiation, the RIA self-compensating effect in SFS based on photo-bleaching was found. The experimental results indicated that the attenuation at pump band plays a significant role in the output power variation and the mean-wavelength shift, the kinetics model of SFS output spectra variations was made. With feedback control pump drive

*Project supported by the Special Fund for Development of National Major Scientific Instruments of China (Grant No. 2013YQ04081504) and the Program for Innovative Research Team in University, China (Grant No. IRT 1203).

†Corresponding author. E-mail: yhyang@buaa.edu.cn

© 2014 Chinese Physical Society and IOP Publishing Ltd

circuitry, a double-pass backward (DPB) configuration with a wavelength selective reflector (WSR) and an edge filter, we demonstrated a DPB-SFS with good radiation-resistant performance.

2. Experimental investigation

Figure 1 shows a compact configuration of SFS, WDM and ISO represent wavelength division multiplexer and optical isolator respectively. 980-nm laser diode (LD) was used as pump source. Pump light was launched into the EDF through the 980/1550 nm WDM and the backward spontaneous emission light passing through the ISO was output. The length of EDFs (M12 from Fibercore Corp.) is about 10 m and its main characteristics are summarized in Table 1.

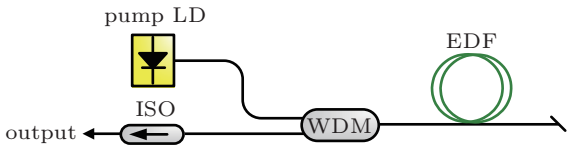


Fig. 1. (color online) Compact configuration SFS.

Table 1. Main characteristics of the EDF.

Parameter	Specification
Absorption@1530 nm/(dB/m)	18.8
Absorption@980 nm/(dB/m)	11.5
Mode field diameter@1550 nm/μm	6.1
Cut-off wavelength/nm	930
Fiber diameter/μm	125.1
Numerical aperture	0.22
Coating diameter/μm	245.9
Coating material	dual acrylate

Before radiation, the backward output spectrum was first measured at different drive currents applied to the pump LD, as shown in Fig. 2(a). The optical powers from the pump LD are about 45 mW and 100 mW at pump drive currents of 100 mA and 200 mA respectively, the relationship between the pump power and the pump current is linear within this range. Taking the spectrum at 200 mA as reference, the spectra variations at different drive currents with respect to this reference level are calculated from the spectra in Fig. 2(a), as shown in Fig. 2(b). It can be seen that the greatest variation occurs at the wavelength band around about 1560 nm and there is also significant variation at around 1532 nm.

During the radiation experiment, only the EDF was placed in the gamma-ray radiation chamber. In EDFs, the fiber core and the coating are used to guide the lightwave and strengthen the fiber, respectively. The gamma-ray has a very strong force of penetration and the coating cannot alleviate the irradiation damage to the fiber core, so the effect of the coating materials and dimensions of the EDF can be ignored. Thus here we consider the overall influence of gamma-ray radiation on the EDF. The radiation dose rate was about 1 rad/s with a total dose of about 36 krad. The LD's drive current was maintained at 200 mA. The spectra were recorded every 2 h and the results are shown in Fig. 3(a). Obviously, the spectrum loss increases with the increase of radiation dose and the longer wavelength band suffers greater loss. This results in a shift of the mean-wavelength toward shorter wavelength with a coefficient of about −114.3 ppm/krad and a total power reduction of more than 60%.

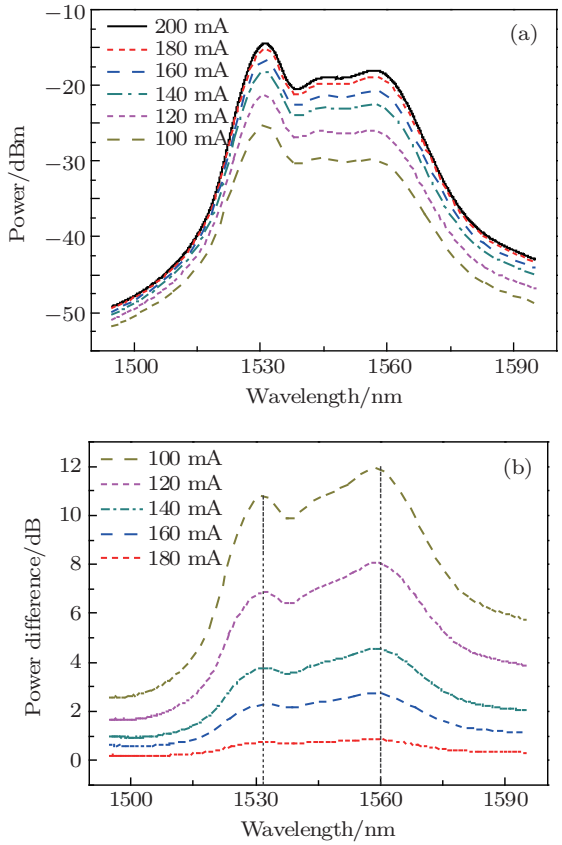


Fig. 2. (color online) (a) SFS spectra at different drive currents of the pump LD. (b) Spectra variations with respect to the reference spectrum at the pump current of 200 mA.

Taking the spectrum before radiation as reference, we calculated the radiation-induced spectrum attenuation by subtracting the spectrum at various radiation dose (Fig. 3(a)) from the spectrum before radiation. The results are shown in Fig. 3(b). We can see that the greatest loss occurs around 1562 nm, the spectrum around 1532 nm is relatively insensitive to radiation and it may be a good wavelength band for space applications. In the EDF, the RIA at the pump and signal bands may both affect the output spectrum when the SFS is working under radiation condition. However, a comparison of the results in Figs. 2(b) and 3(b) reveals that the variations of the spectra are of similar shapes and the peak wavelengths of different spectra are both at around 1560 nm. This suggests that the attenuation at the pump band increases significantly

when the radiation dose increases, and this might be the main cause of the induced spectrum change as well as total power change in the SFS.

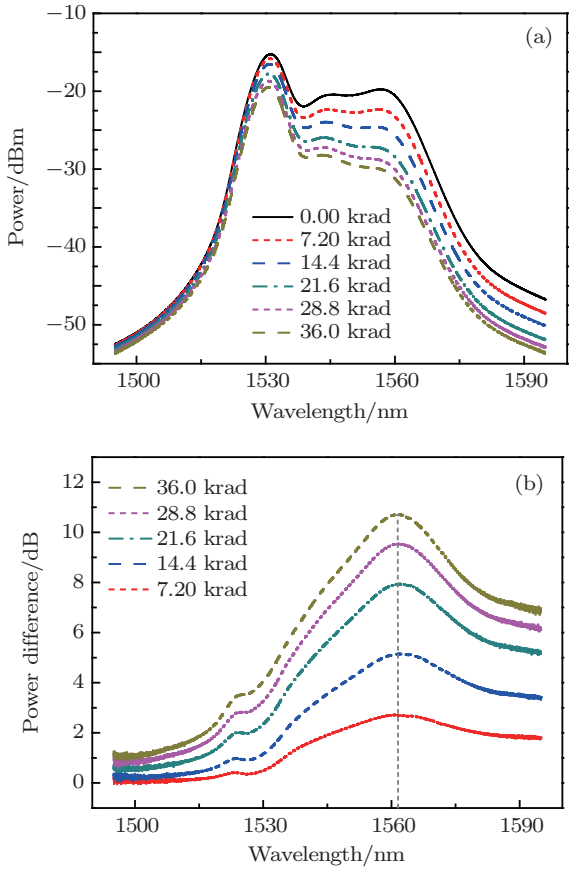


Fig. 3. (color online) (a) SFS spectra at different radiation dose, (b) spectra variations with respect to the reference spectrum of zero radiation dose. The LD's drive current was set to be 200 mA.

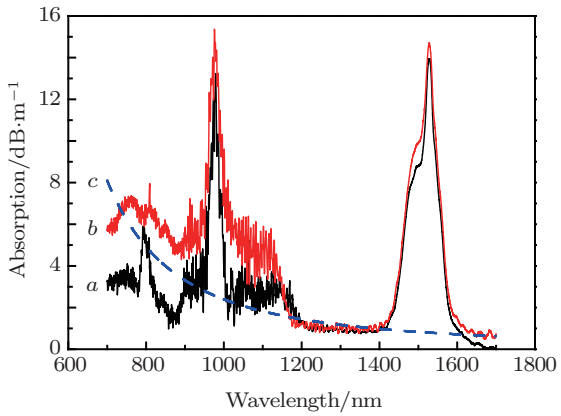


Fig. 4. (color online) The absorption spectrum of EDF, curves *a*, *b*, *c* mean before irradiation, after irradiation (dose about 36 krad), fitted background attenuation, respectively.

To better understand the reason for induced spectra variations, we measured the absorption spectrum of EDF used in our experiments. A super-continuum white light source (SuperK Compact, Koheras Inc.) with spectral range from 500 nm to 2400 nm and total power about 100 mW was used as the broadband source, the optical spectrum analyzer (OSA) (AQ6370, Yokogawa Inc.) was used to monitor the transmitted light spectrum after a 10-m EDF. The super-continuum white light source uses multimode fiber as output coupling fiber and little power can be injected into the single mode EDF, so the white light power density in EDF is weak and cannot induce nonlinear effects. The absorption spectra of the EDF used in the SFS before and after irradiation are shown in Fig. 4. The attenuation increases greatly at pump band after irradiation and the RIBA is about 3.24 dB/m at the pump wavelength of 974.12 nm. There is little change observed in RIBA around 1550-nm band. Curve *c* in Fig. 4 is the fitted background attenuation spectrum with the model given as[15]

$$\alpha(\lambda) = \frac{(\lambda_c - \lambda_0)^2 \cdot c\phi^{1-f} D^f}{(\lambda - \lambda_0)^2}, \tag{1}$$

where λ_0 is the parameter that gives a rough estimation of the absorption peak position, λ_c is concerned wavelength, c and f are temperature-dependent parameters, ϕ is irradiation dose rate, and D is the total deposited dose. From our experiment results, the fitted λ_0 is 353.9 nm and agrees well with the model. RIBA is due to the generation of color center with absorption peak generally lying in the ultraviolet region. It is wavelength dependent and can be described with a Lorentzian curve in which the attenuation decreases from the visible to the infrared part of the spectrum.[15,16] With this model, the calculated RIBA at pump band is about twice of that at signal band under about 36-krad dose and increases faster with the increment of total radiation dose. Considering the output spectrum of a SPB-SFS (Fig. 3(a)), its strong gain hump is near 1530-nm band and the gain near 1560 nm increases due to the reabsorption of the backward ASE light by Er^{3+} in the front of the EDF. When the EDF is under gamma-ray irradiation, the backward ASE light power decreases dramatically due to the great RIBA of pump light. It reduces the reabsorption and the gain near 1560 nm is insufficient to support the right hump of the spectrum, which leads to the final output spectra variations shown in Fig. 3(a).

The aforementioned analysis demonstrated that the RIBA at pump band plays a significant role on the output power and spectra variations. By appropriately increasing the LD's driving current, the pump power in the EDF could be kept at a suitable level to actively compensate the RIBA at pump band and the RIBA of the EDF could be intensely photo-bleached by 980-nm pump laser to achieve a SFS with better spectrum stability, which is the RIA self-compensating effect in SFS.

3. General mathematical model

In Ref. [10], Peng T S reported photo-annealing (namely photo-bleaching) effects on gamma radiation induced attenuation in EDF and the sources using 532 nm and 976 nm

photo-annealing lasers. From the experiment results, we can draw a conclusion that the photo-bleaching effect can be regarded as the inverse process of RIBA and it shares the same mathematical model. The self-compensating capability due to photo-bleaching is wavelength dependent and proportional to the pump power. It can be enhanced by multi-wavelength pumps and its mathematical model can be described as

$$\beta(\lambda) = \sum_{\lambda_p} \frac{(\lambda_p - \lambda_0)^2 \cdot c' p_p^{1-f'}}{(\lambda - \lambda_0)^2}, \quad (2)$$

where λ_p and p_p are the pump wavelength and power, respectively; c' and f' are temperature-dependent parameters affecting the photo-bleaching efficiency.

Considering the ASE spectrum region (C band), the spectrum power attenuation at the wavelength λ due to RIBA can be calculated with Eq. (1), which decreases with the increment of λ. The recovery of spectrum power attenuation at the wavelength λ due to photo-bleaching effect can be calculated with Eq. (2). It decreases with the increment of λ and increases with the increment of p_p. By subtracting Eq. (2) from Eq. (1), we can get the spectrum power attenuation at the wavelength λ when SFS is under radiation condition

$$\Delta P(\lambda) = \frac{(\lambda_c - \lambda_0)^2 \cdot c\phi^{1-f} D^f - \sum_{\lambda_p} (\lambda_p - \lambda_0)^2 \cdot c' p_p^{1-f'}}{(\lambda - \lambda_0)^2}. \quad (3)$$

This general mathematical model describes the RIBA and self-compensating effect in SFS, which implies that the RIA could be mostly self-compensated when ϕ is small and p_p is appropriately adjusted.

4. Design and test of a radiation-resistant SFS

Based on the findings in Section 2 and the model in Section 3, a radiation-resistant DPB-SFS is designed and illustrated in Fig. 5. WSR with the reflection spectrum shown in Fig. 6(a) in coupled with an edge filter with the transmission spectrum given in Fig. 6(b) define the output spectrum of the SFS. The pump LD peak wavelength is 974 nm. In this SFS, the forward spontaneous emission is reflected by the WSR and the reflected spectrum is modified. The reflected and backward spontaneous emission from the WDM further passes through the edge filter. The final output spectrum has a Gaussian profile with 3-dB bandwidth of about 7 nm, as shown in Fig. 6(c). In this scheme, the long wavelength band signal was filtered out to reduce the RIABA of EDF and obtain a more stable output spectrum. The center wavelength of the SFS was chosen to be at around 1532 nm because the radiation-induced spectrum change is relatively small and may be easily compensated by reasonable adjustment of the pump current. An integrated power monitor (IPM) with thin film beam splitter and photo-detector (shown in sub-figure of Fig. 5) was employed to pick about 5% of output power as feedback signal to control the pump LD drive current with the drive & control circuitry, which can provide sufficient pump energy to the EDF in radiation environment. The DPB configuration can also provide higher light energy density in EDF to enhance the photo-bleaching effect greatly.

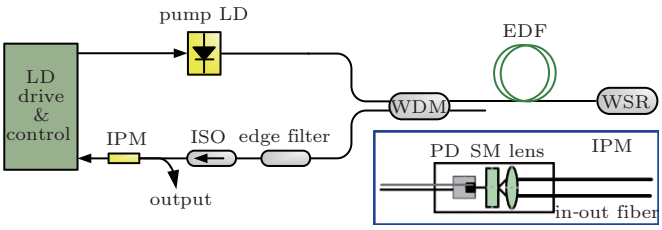


Fig. 5. (color online) Radiation-resistant SFS configuration.

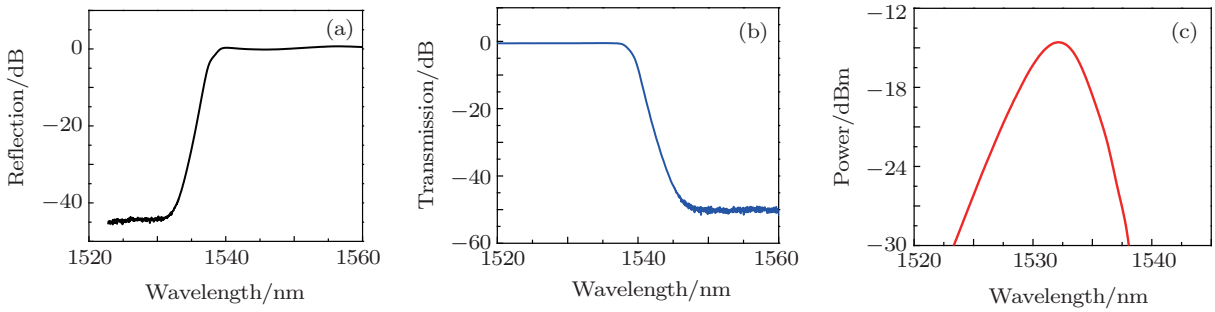


Fig. 6. (color online) (a) Reflection spectrum of WSR, (b) transmission spectrum of the edge filter, (c) final output spectrum of the SFS.

The SFS shown in Fig. 5 was tested under gamma-ray radiation. The experiment was performed with ^{60}Co radiation source. The radiation dose rate is less than 0.1 rad/s with the total dose of about 200 krad, the environment temperature is about 25 °C. The output spectrum and power were recorded by AQ6370 OSA and optical power meter (ILX FPM-8210H, ILXLightwave Inc.), respectively.

The output spectra of SFS at different radiation dose are illustrated in Fig. 7(a). The curves overlap greatly because the spectra variations are very small. The SFS has an output power

of over 10 mW and power instability of less than 5% after irradiation of 200 krad. Figure 7(b) shows the mean-wavelength changes of the SFS during radiation. It is noticed that the mean-wavelength shifts toward shorter wavelength with a very small slope and about 87.4 ppm mean-wavelength variation was achieved after irradiation of 200 krad.

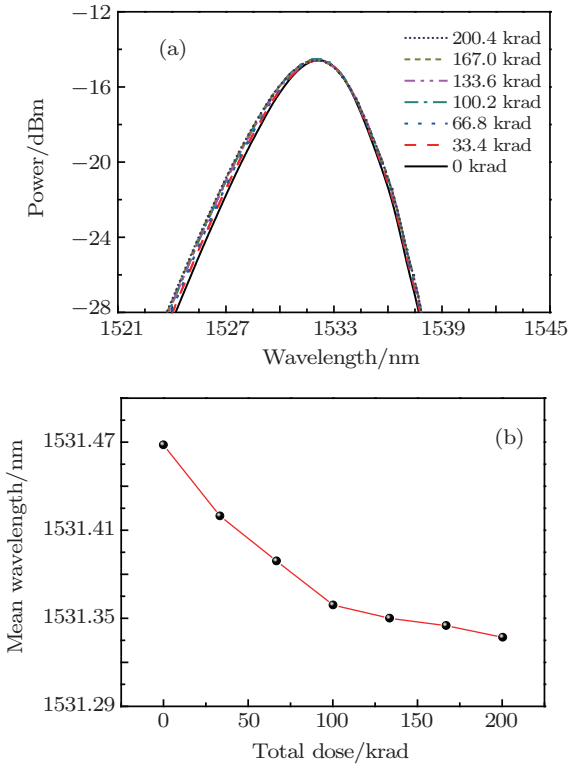


Fig. 7. (color online) (a) SFS spectrum at different radiation dose, (b) SFS mean-wavelength variation as function of radiation dose.

In the radiation experiment, it can be seen that the mean-wavelength of the SFS still somewhat shifted even using these radiation-resistant technologies, which may be due to the residual RIABA of the EDF that can still influence the emission spectrum.

5. Conclusion

The SFS output spectra variations at different pump currents and under different doses of gamma-ray radiation were measured and compared, respectively. The radiation-induced RIA self-compensating effect in SFS based on photobleaching was found and a general mathematical model of SFS output spectrum attenuation was derived. We identified that the RIBA at pump wavelength was the main cause of the total output power and spectra variations, which can be compensated by active control of the pump power to enhance the self-compensating effect. With closed-loop feedback control of pump current and spectrum re-shaping technology, a DPB-SFS prototype with output power of over 10 mW was made and tested under ^{60}Co irradiation environment. The experimental results demonstrated that the SFS could achieve a mean-wavelength stability of about 87.4 ppm and an output power instability of less than 5% under total gamma-ray irradiation dose of 200 krad (Si). This research provides a practical source technology for high stability, radiation-resistant FOG and related systems. The related technologies may be useful for other fiber components such as EDFAs and fiber lasers based on other rare-earth-doped fibers when applied in space environment.

References

[1] Wysocki P F, Digonnet M J F, Kim B Y and Shaw H J 1994 *J. Lightw. Technol.* **12** 550
[2] Friebele E J, Askins C G, Miller G A, Peele J R and Wasserman L R 2004 *Photonics for Space Environments IX,* August 2–3, 2004 Denver, United States, p.120
[3] Ma J, Li M, Tan L Y, Zhou Y P, Yu S Y and Ran Q W 2009 *Opt. Express* **17** 15571
[4] Friebele E J and Gingerich M E 1981 *Appl. Opt.* **20** 3448
[5] Park H G, Digonnet M and Kino G 2003 *J. Lightw. Technol.* **21** 3427
[6] Suo X X, Yang Y H, Yang M W, Shi X W and Zhao S J 2010 *Advanced Sensor Systems and Applications IV,* October 18–20, 2010 Beijing, China, p. 78533Z
[7] Zotov K V, Likhachev M E, Tomashuk A L, Bubnov M M, Yashkov M V and Guryanov A N 2007 *J. Quantum Elect.* **37** 946
[8] Zotov K V, Likhachev M E, Tomashuk A L, Bubnov M M, Yashkov M V, Guryanov A N and Klyamkin S N 2008 *Trans. Nucl. Sci.* **55** 2213
[9] Michal R J, Lam L K and Rozelle D M *U. S. Patent* 6025915 [2000-02-15]
[10] Peng T S, Huang Y W, Wang L A, Liu R Y and Chou F I 2010 *Trans. Nucl. Sci.* **57** 2327
[11] Zotov K V, Likhachev M E, Tomashuk A L, Kosolapov A F, Bubnov M M, Yashkov M V, Guryanov A N and Dianov E M 2008 *IEEE Photon. Technol. Lett.* **20** 1476
[12] Peng T S, Wang L A and Liu R Y 2011 *IEEE Photon. Technol. Lett.* **23** 1460
[13] Peng T S and Wang L A 2012 *IEEE Photon. Technol. Lett.* **24** 1340
[14] Williams G M, Wright B M, Mack W D and Friebele E J 1999 *Optical Fiber Reliability and Testing,* September 19–20, 1999 Boston, MA, USA, p. 271
[15] Berne O, Caussanel M and Gilard O 2004 *IEEE Photon. Technol. Lett.* **16** 2227
[16] Rose T S, Gunn D and Valley G C 2001 *J. Lightw. Technol.* **19** 1918
[17] Jin J, Wang X Q, Lin S and Song N F 2012 *Chin. Phys. B* **21** 094220